

Commissioning of the High Current Ion Sources at the New GSI Injector (HSI)

H. Reich, F. Heymach, P. Spädtke

Gesellschaft für Schwerionenforschung mbH (GSI), Planckstr. 1, D-64291 Darmstadt, Germany

Abstract

The new high current injector consisting of an RFQ and an IH structure accepts ions with a mass-to-charge ratio m/q up to 65 with a space charge limit of $0.25 \text{ emA} \times m/q$. Two types of high current ion sources are used to deliver ion beam currents up to the space charge limit of the RFQ. As a source for ions of gaseous elements a multi cusp ion source (MUCIS) [1] was used. Metallic ions were produced by a metal vapor vacuum arc ion source (MEVVA) [2] [3]. A main concern of the sources is the reliability and the stability of the extracted ion beam. In addition the splitting of the total voltage required to achieve the injection energy of 2.2 keV/u (extraction voltage and acceleration voltage) was found to have a strong influence on the beam matching.

1 INTRODUCTION

The large number of experiments performed at the heavy ion accelerator facilities at GSI are demanding a great variety of different ion species and beam intensities. In 1999 the old Wideröe structure of the GSI UNILAC has been replaced by a new RFQ/IH structure, the high current injector (HSI) [4]. With the new accelerator the intensities of ion beams to be injected into the heavy ion synchrotron (SIS) are planned to be increased especially for heavy ions (design ion: U^{4+}) by two orders of magnitude [5]. The low energy beam line (LEBT) [6] as well as the ion sources had to be modified to meet the new injection conditions of the HSI: ion beams with lower injection energy, lower ion charge state and higher intensities with emittances adjusted to the RFQ acceptance have to be produced. Mainly the MUCIS was used to deliver an Ar^{1+} ion beam. The very stable operation of the MUCIS and an ion beam intensity well above the theoretical space charge limit of the RFQ, provided at the front of the RFQ, enabled ideal conditions for the commissioning of the new accelerator.

2 HIGH CURRENT ION SOURCES AND LOW ENERGY BEAM LINE

The High Current Terminal was operated alternatively with a MUCIS or a MEVVA ion source.

In fig. 1 the low energy beam transport line (LEBT) [6] is shown together with the high current ion sources, preacceleration and beam diagnostics. Typical measured intensities are listed in tab. 1. As an example Fig. 2 and Fig. 3 show Ni^{1+} beam pulses (MEVVA) measured with beam transformers [8] along the low energy beam line. Fig. 2 shows the complete ion beam pulse, whereas in fig. 3 one typical MEVVA instability appears in all beam transformer signals shifted by the time of flight of the ions. From such

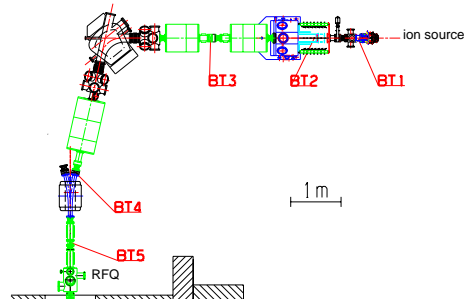


Figure 1: Low Energy Beam Line and ion beam diagnostics.

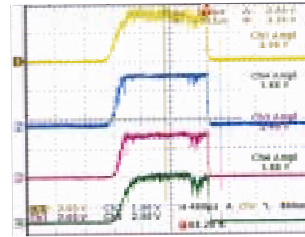


Figure 2: Ni^{1+} (MEVVA) measurement along the low energy beam transport line, complete ion beam pulse, hor. scale: $400 \mu\text{s}/\text{div}$. ch 1: BT2, total preaccelerated ion beam current, ch 2: BT3, total ion beam current transported through the first quadrupole-triplet, ch 3: BT4, separated Ni^{1+} ion beam (after dipole magnet), ch 4: BT5, transported Ni^{1+} ion beam at RFQ injection.

a measurement possible amplifications of ion beam noise during transport could be determined. For the given frequency modulation no influence of the noise on the beam transport could be found. In fig. 4 typical measured ion beam pulses are displayed for uranium (MEVVA) and argon (MUCIS) in comparison.

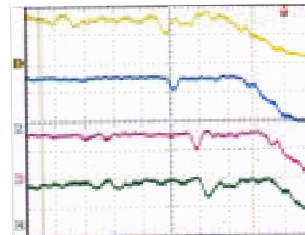


Figure 3: Ni^{1+} (MEVVA) measurement along the low energy beam transport line: short part of the ion beam pulse, MEVVA instabilities shifted by time of flight, hor. scale: $10 \mu\text{s}/\text{div}$. ch 1: BT2, total preaccelerated ion beam current, ch 2: BT3, total ion beam current transported through the first quadrupole-triplet, ch 3: BT4, separated Ni^{1+} ion beam (after dipole magnet), ch 4: BT5, transported Ni^{1+} ion beam at RFQ injection.

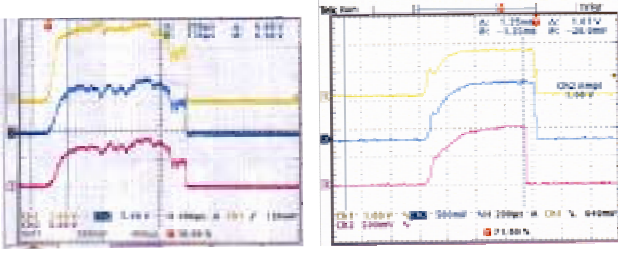


Figure 4: typical ion beam pulses; left: Mevva (uranium), right: MUCIS (argon) ch1: BT3, 26mA total current uranium (left); 22mA total current argon (right) ch2: BT4, 8.8mA U^{4+} ; 18.8mA Ar^{1+} (right) ch3: BT5, 7.8mA U^{4+} (left); 18.3mA Ar^{1+} (right)

Table 1: Ion beam currents, measured with beam transformers [7] at different places along the low energy transport beam line: BT1: total ion beam current extracted from the ion source (on Terminal potential), BT3: current of preaccelerated ion beam after the gap on ground potential, BT5: charge state separated ion beam current in front of RFQ.

	MUCIS	MEVVA
BT1 [emA]	80-100	80-100
BT3 [emA]	$Ar^{1+,2+} \approx 35$	$Ti^{1+,2+} \approx 20$ $Ni^{1+,2+} \approx 25$ $U^{3+,4+,5+} \approx 28$
BT5 [emA]	$Ar^{1+} : 16-20$	$Ti^{1+} \approx 3$ $Ni^{1+} \approx 10$ $Ni^{2+} \approx 2$ $U^{4+} : 6-10$

3 EMITTANCE MEASUREMENTS

Beside the required beam intensities, the ion sources have to deliver an ion beam with an emittance in horizontal and in the vertical plane matched to the acceptance of the RFQ ($140 \text{ mm mrad} [\text{area}/\pi]$). The emittance measurements were performed at the place of injection into the RFQ. Two different techniques were used: the emittance was measured with a combination of a movable slit with a beam profile grid and with a "Pepper-Pot", where a single ion beam pulse, going through an area of small holes, produces an image on a screen, which can be analyzed by a CCD camera. Both techniques are fully automatized and computer-controlled. For detailed information of the experimental setup see [7], [8] and the references therein. At an ion beam energy of 2.2 keV/u , Fig. 5 shows emittance measurements performed in the horizontal and the vertical plane for Ar^{1+} (MUCIS) and Ni^{1+} (MEVVA). All measured emittances are within the theoretical calculated RFQ acceptance.

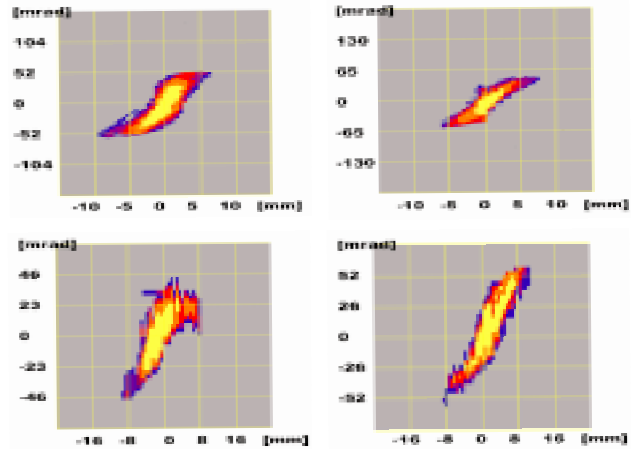


Figure 5: Emittance measurements : top: MUCIS: Ar^{1+} , ion beam current: $\approx 16 \text{ emA}$; bottom: MEVVA ion source: Ni^{1+} , ion beam current: $\approx 10 \text{ emA}$; (left: horizontal plane, right: vertical plane)

4 ION BEAM EXTRACTION AND PREACCELERATION

It turned out that the low injection energy of the RFQ made it difficult to transport high current ion beams extracted from the ion sources without losses. The fixed injection energy of 2.2 keV/u has to be divided into extraction voltage and terminal voltage. As the extraction voltage has to be matched to the plasma density in the ion source to obtain a maximum extracted ion beam current, it was necessary to install a variable acceleration gap (fig. 6) to match the focusing strength to the ion beam current. Fig. 7 shows the

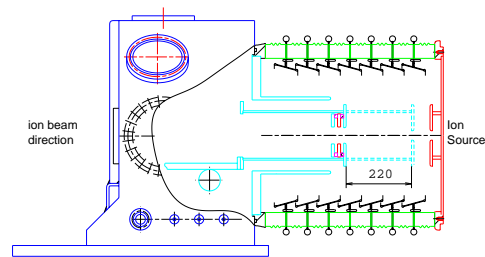


Figure 6: Moveable single gap: gap width adjustable from 30 to 250 mm

transmission (in this case: $Ar^{1+,2+}$) through the gap and the first magnetic quadrupole-triplet as function of the gap width. It can clearly be seen that a optimized transmission can be obtained at a specific gap width. This optimization of the gap width has to be done for each ion species and for each current. However, the absolute value of the transmission reached in this part of the ion beam line was only about 50% and has to be improved. To overcome this problem, computer simulations of the ion beam transport in the accelerating gap are performed (AXCEL-INP, KOBRA 3-INP [9]) to optimize the gap geometry and to study the influence of beam focusing by an additional solenoid

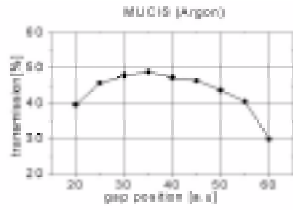


Figure 7: Transmission measurement of the transported total ion beam current through the gap and the first magnetic quadrupole triplet as function of the gap width.

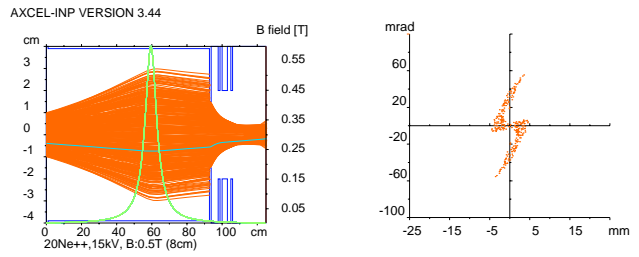


Figure 10: Ne²⁺ ion beam simulation: transport through the gap (solenoid: 0.5 Tesla / 4cm); left: trajectories, right: emittance

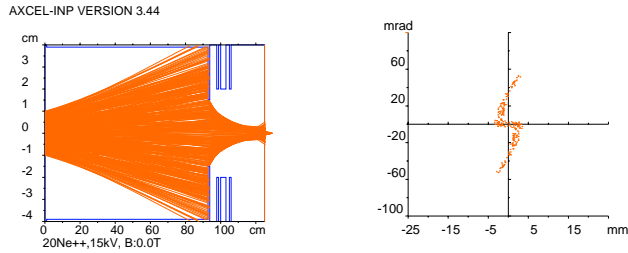


Figure 8: Ne²⁺ Ion beam simulation: transport through the gap (no focusing by solenoid); left: trajectories, right: emittance)

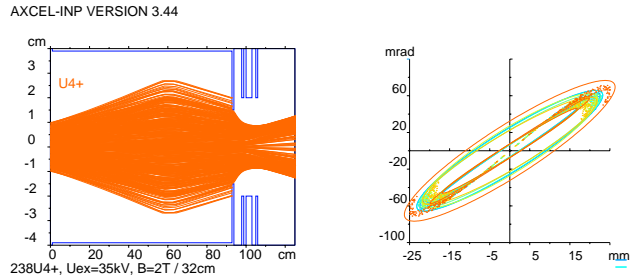


Figure 11: U⁴⁺ ion beam simulation: transport through the gap (solenoid: 2.0 T / 16cm); left: trajectories, right: emittance ≤ 120 mm mrad

between the ion source extraction and the gap. The simulations have been made with the assumption that the beam is space charge compensated throughout the drift from the ion source to the gap and behind the screening electrode after acceleration. Typical measured ion beam currents and charge state distributions have been taken as input parameters. The space charge forces inside the gap were taken into account. In fig. 8 and fig. 10 the results of two simulation calculations are shown: fig. 8 shows in trajectories the transport through the gap of a Ne ion beam without additional focusing by a solenoid magnetic field, fig. 10 shows the transport with optimized magnetic focusing. The emittancies at the right side of fig. 10 and fig. 8 are calculated at a distance of 120cm from the extraction system and appr. 20cm behind the gap. First experiments were performed using an existing solenoid (max. field strength on axis: 0.6 Tesla / 40mm) and ion beams of He and Ne (MUCIS). With an optimized magnet field a significant increase of transmission could be achieved (fig. 9) in good agreement with the simulation. On the basis of these experimental data and simulation results, first calculations were performed to improve the transport for U⁴⁺. As a result

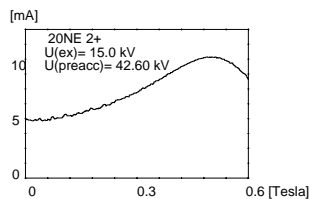


Figure 9: Experimental data: ion beam current (Ne²⁺) as function of the magnetic field strength (solenoid). horizontal: magnetic field strength of solenoid (0.0T to 0.6T), vertical: ion beam current [mA].

fig. 11 shows the transport of an U⁴⁺ ion beam through the accelerating gap with solenoid magnetic focusing. The preliminary optimized magnetic field was found to have a magnetic field strength of about 2 Tesla on axis and a half width length of about 32 cm. The calculated emittance was found in this case to be smaller than 120mm mrad. The aberrations, which can be seen in fig. 11 can be minimized by a carefully adjustment of the ion beam focus inside the gap.

5 REFERENCES

- [1] R. Keller Multicharged ion production with MUCIS, GSI annual report 1987, p. 360
- [2] I.G. Brown, The Metal Vapor Vacuum Arc Ion Source, in The Physics and Technology of Ion Sources, ed. by I.G. Brown, John Wiley and Sons, New York, 1989
- [3] H. Reich, E.M. Oks, P. Spädtke, MEVVA Ion Source development at GSI, Rev. Sci. Instrum. **71**(2), 707 (2000)
- [4] W. Barth, Commissioning of the 1.4MeV/u High current Heavy Ion LINAC at GSI, this proceedings
- [5] P. Spädtke et.al., Ion Source development at GSI, Rev. Sci. Instrum. **69**(2), 1079 (1998).
- [6] L. Dahl, The Low Energy Beam Transport System of th New GSI High Current Injector, this proceedings
- [7] P. Strehl et.al. Emittance measurements at the new UNILAC Pre-Stripper, DIPAC, Chester, U.K., 1999
- [8] B. Wolf (ed.) Handbook of Ion Sources, CRC Press, Boca Raton 1995, p. 385.
- [9] INP Junkerstr.99, 65205 Wiesbaden, Germany